Title

Regional and Voxel-Wise Comparisons of Blood Flow Measurements Between Dynamic Susceptibility Contrast Magnetic Resonance Imaging (DSC-MRI) and Arterial Spin Labeling (ASL) in Brain Tumors

Journal

Journal of Neuroimaging, 24(1)

ISSN

1051-2284

Authors

White, Carissa M
Pope, Whitney B
Zaw, Taryar
et al.

Publication Date

2014

DOI

10.1111/j.1552-6569.2012.00703.x

Peer reviewed

Clinical Investigative Study

Regional and Voxel-Wise Comparisons of Blood Flow Measurements Between Dynamic Susceptibility Contrast Magnetic Resonance Imaging (DSC-MRI) and Arterial Spin Labeling (ASL) in Brain Tumors

Carissa M. White, BA, Whitney B. Pope, MD, PhD, Taryar Zaw, BS, Joe Qiao, MD, Kourosh M. Naeini, MD, Albert Lai, MD, PhD, Phioanh L. Nghiemphu, MD, J.J. Wang, PhD, Timothy F. Cloughesy, MD, Benjamin M. Ellingson, PhD

From the Department of Radiological Sciences, David Geffen School of Medicine, University of California Los Angeles, Los Angeles, CA 90095 (CMW, WBP, TZ, JQ, KMN, JJW, BME); Department of Neurology, David Geffen School of Medicine, University of California Los Angeles, Los Angeles, CA 90095 (AL, PLN, JJW, TFC).

ABSTRACT

The objective of the current study was to evaluate the regional and voxel-wise correlation between dynamic susceptibility contrast (DSC) and arterial spin labeling (ASL) perfusion magnetic resonance imaging (MRI) measurement of cerebral blood flow (CBF) in patients with brain tumors. Thirty patients with histologically verified brain tumors were evaluated in the current study. DSC-MRI was performed by first using a preload dose of gadolinium contrast, then collecting a dynamic image acquisition during a bolus of contrast, followed by posthoc contrast agent leakage correction. Pseudocontinuous ASL was collected using 30 pairs of tag and control acquisition using a 3-dimensional gradient-echo spin-echo (GRASE) acquisition. All images were registered to a high-resolution anatomical atlas. Average CBF measurements within regions of contrast-enhancement and T2 hyperintensity were evaluated between the two modalities. Additionally, voxel-wise correlation between CBF measurements obtained with DSC and ASL were assessed. Results demonstrated a positive linear correlation between DSC and ASL measurements of CBF when regional average values were compared; however, a statistically significant voxel-wise correlation was only observed in around 30-40% of patients. These results suggest DSC and ASL may provide regionally similar, but spatially different measurements of CBF.

Keywords: Perfusion, glioblastoma, MRI, DSC, ASL, brain tumor.

Acceptance: Received August 22, 2011, and in revised form November 4, 2011. Accepted for publication December 15, 2011.

Correspondence: Address correspondence to Benjamin M. Ellingson, PhD, Department of Radiological Sciences, David Geffen School of Medicine, University of California Los Angeles, 924 Westwood Blvd., Suite 615, Los Angeles, CA 90024. E-mail: bellingson@mednet.ucla.edu.

J Neuroimaging 2014;24:23-30.
DOI: 10.1111/j.1552-6569.2012.00703.x

Introduction

Magnetic resonance imaging (MRI) is the mainstay of brain tumor imaging, both in diagnosis and treatment. Traditionally, clinicians rely on contrast enhancement to characterize the relative degree of malignancy in suptratentorial tumors. However, with increasing evidence for the critical role of angiogenesis in determination of tumor malignancy and growth potential, imaging modalities capable of quantifying cerebral blood flow (CBF) have become attractive alternatives. Several studies have shown that higher grade brain tumors have significantly higher perfusion measurements than low-grade tumors,[1-3] suggesting that CBF measurements may be a better method for characterizing brain tumor angiogenesis and monitor treatment response. As antiangiogenic therapy is now the standard of care for recurrent malignant gliomas, there is a significant need for monitoring changes in cerebral blood flow within areas of suspected tumor independent of contrast enhancement.

The gold standard for perfusion MR imaging is dynamic susceptibility contrast (DSC) MRI, which uses a bolus injection of paramagnetic contrast agent, usually gadolinium, as a nondiffusible tracer for CBF. Calculations of CBF, CBV (cerebral blood volume; the fraction of tissue volume occupied by blood), and mean transit time (MTT = CBF/CBV, the time it takes for blood to pass through the vasculature within the tissue of interest) can be made simultaneously. However, this requires deconvolving the arterial input function (AIF) from the time series data. As a result, few studies have been done on the reproducibility of DSC measurements of CBF.

Arterial spin labeling (ASL) is a continually evolving noninvasive technique for quantifying CBF. ASL uses magnetically tagged blood water as an endogenous, diffusible tracer for blood flow. Specifically, blood in a feeding artery is subjected to an inversion pulse, and the magnetization can be followed as it is transferred to brain tissue by capillary exchange at a rate dependent on perfusion of the tissue. Subtracting the image taken prior to labeling (the control) yields a "perfusion weighted" image, representing only the transported magnetization from blood flow. Because it eliminates the need for exogenous contrast, ASL has the inherent advantage of being able to perform serial scans to track tumor growth and/or drug response, as well

as use in pediatric patients, and patients with renal failure. ASL has been shown to accurately measure CBF in normal healthy volunteers, and to be robust in brain regions with normal and rapid arrival times. This makes it a potentially valuable modality for monitoring treatment response in hyperperfused brain tumors.

Previous studies have shown that DSC and ASL yield comparable perfusion values in normal brain tissue[4] and in a limited number of tumors[5-7]; however, regional and voxel-wise comparisons of CBF measurements between DSC and ASL are lacking in the current literature. The purpose of the current study was to compare CBF measurements obtained from DSC and ASL techniques in patients with brain tumors and define the relationship between values obtained by each modality.

Materials and Methods

Patient Population

Thirty ($n = 30$) patients with histologically verified primary gliomas ($n = 22$), primary CNS lymphoma ($n = 2$), and cerebral metastases ($n = 6$) were evaluated in the current study. Of the patients with primary gliomas, a total of 13 patients had a glioblastoma (WHO IV), 1 patient had a gliosarcoma (WHO IV), 2 patients had an anaplastic astrocytoma, 1 patient had an anaplastic oligodendroglioma, 3 patients had a mixed anaplastic oligoastrocytoma, and 2 patients had a low-grade oligoastrocytoma. Of the patients with cerebral metastases, 2 patients had metastatic melanoma, 1 patient had metastatic synovial sarcoma, 1 patient had metastatic hepatocellular carcinoma, 1 patient had metastatic adenocarcinoma, and 1 patient had metastatic carcinoma. The mean patient age was 57.3 years, with 19 male patients and 11 female patients. This study was approved by the UCLA Institutional Review Board and all participants signed informed consent to be included in our neuro-oncology database. All applicable Health Insurance Portability and Accountability Act (HIPPA) regulations were adhered to during data acquisition. The study images were conducted from November 2010 through May 2011.

Magnetic Resonance Imaging

Imaging studies were performed using a Siemens 1.5 T Avanto or 3.0 T Trio MR scanners (Siemens Healthcare, Erlangen, Germany) using a standard head coil. Each patient received routine clinical MRI scans, including a precontrast T1-weighted (T1) scan, postcontrast T1-weighted (T1+C) scan, T2-weighted scan, fluid-attenuated inversion recovery (FLAIR) scan, and a diffusion weighted (DWI) scan.

Dynamic Susceptibility Contrast (DSC)-MRI

A .025 mmoL/kg preload dose of a gadolinium contrast agent was administered prior to DSC acquisition to diminish contrast agent extravasation.[2,8,9] Following the preload, a bolus of gadopentetate dimeglumine (Gd-DTPA; Magnevist®, Bayer Schering Pharma AG, Leverkusen, Germany), administered at a dose of 10-20 cc (.075 mmoL/kg) at a rate of 3-5 cc/second using a power injector, was used for DSC acquisition and subsequent post contrast T1 weighted images (total of .1 mmoL/kg). DSC scan parameters included echo times (TE) ranging from 23 to 50 ms, repetition times (TR) ranging from 1,250 to 1,400 ms, flip angles (FA) ranging from 30 to 35 degrees, 40 to 90 repetitions (temporal time points), slice thickness ranging from 4 to 7 mm with interslice gap ranging from 0 to 1.5 mm, number of slices ranging from 6 to 20, and matrix size ranging from 80 × 96 to 128 × 128, depending on whether perfusion data were acquired on a 1.5 T or 3.0 T system.

Data analysis of DSC data was performed offline using commercially available postprocessing software (IB Neuro v2.0™; Imaging Biometrics, LLC, Elm Grove, WI, USA). DSC analysis consisted of the following steps: (1) truncation of the first five time points in the DSC time series, since the MR signal does not reach steady state before this time, (2) calculation of the prebolus signal intensity on a voxel-wise basis, (3) conversion of truncated DSC time series to a concentration-time curve based on the T2* relaxivity of the contrast agent, and (4) estimation of CBV on a voxel-wise basis by using a 120 point trapezoidal integration with correction for leakage, as described in previous publications.[2,8-10] CBF was calculated using circular deconvolution of the arterial input function, which was chosen automatically in five voxels using IB Neuro v2.0™.

Pseudocontinuous Arterial Spin Labeling (PCASL) with 3D GRASE and Background Suppression

An inherent constraint to 2D ASL acquired using echoplanar acquisition is the limited number of obtainable images, reducing the amount of total brain coverage. Additionally, each slice acquired with 2D ASL experiences slightly different inflow time, thus it is difficult to estimate a precise transit time when multiple slices are acquired. The use of 3-dimensional acquisition techniques overcomes many of these limitations, allowing both whole brain coverage and simultaneous acquisition to ensure a unified mean transit time. Pseudocontinuous ASL provides the main advantages of pulsed ASL, including a slightly lower radiofrequency power deposition and higher inversion efficiency, while maintaining the benefits known to continuous ASL, such as the ability to tag spins within a physiological range of velocities and higher overall tagging efficiency. In the current study, ASL PWI scans were performed using a PCASL pulse sequence with background suppressed 3D GRASE (Gradient and Spin Echo) readout (postlabeling delay = 2 second, FOV = 22 cm, matrix = 64 × 64, 26 × 5 mm slices, rate-2 GRAPPA, TR = 4 second, TE = 22 ms, 30 pair of tag and control acquired in 4 minute)[11,12]. Data analysis was performed with Interactive Data Language (IDL (Boulder, CO, USA)) software programs developed in-house. ASL images were corrected for motion, pairwise subtracted between label and control images followed by averaging to generate the mean difference image (ΔM). Quantitative CBF (f) maps were calculated based on the following equation:[11,13]

$$f = \frac{\lambda \Delta M R_{1a}}{2\alpha M_0 [\exp(-w R_{1a}) - \exp(-\tau + w) R_{1a}]} \qquad (1)$$

where R_{1a} (=.72/0.61 second^{-1} at 1.5/3 T) is the longitudinal relaxation rate of blood, M_0 is the equilibrium magnetization of brain tissue, α (= .8) is the tagging efficiency, τ (=1.5 second)

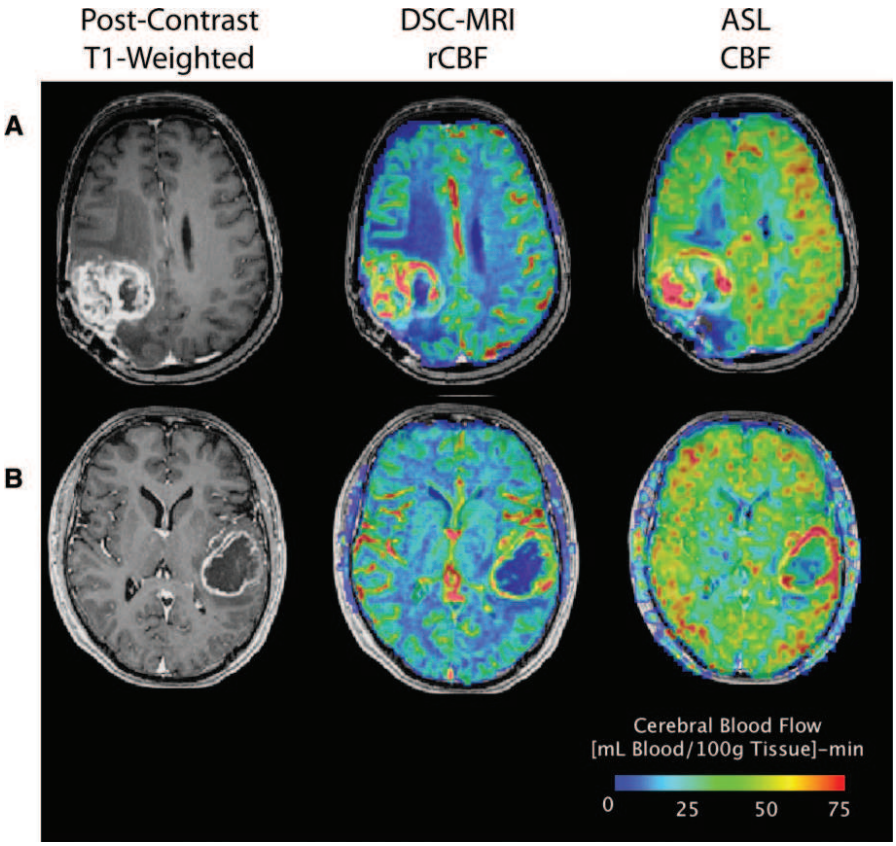

Fig 1. Contrast enhancing and perfusion images in two representative patients with glioblastoma. (A) A patient with recurrent glioblastoma illustrating heterogeneous regions of elevated cerebral blood flow (CBF) for both dynamic susceptibility contrast (DSC) and arterial spin labeling (ASL) perfusion within the contrast-enhancing lesion. (B) A newly diagnosed patient with glioblastoma illustrating relatively high CBF in the left temporal ring enhancing lesion along with characteristically low CBF in central necrotic regions. In both these examples, regions of elevated CBF appear to be spatially different between the two modalities.

is the duration of the labeling pulse, w (=2 second) is the post-labeling delay time, and λ (=0.9 g/mL) is blood/tissue water partition coefficient.[14]

Selection of Regions of Interest (ROIs)

Regions of postcontrast T1 enhancement were selected, as well as regions of T2 ($n = 19$) or FLAIR signal abnormality ($n = 11$), based on RANO recommendations, the observation that infiltration of tumor into normal brain parenchyma usually cause an increase in T2-weighted or FLAIR abnormal signal[15-17] and recommendations from multiple studies suggesting that T2 signal abnormalities should be routinely used to visualize the extent of malignant infiltrating tumor.[18-20] Regions of interest were created using a semiautomated thresholding and region-growing technique described in a previous publication.[21] Additionally, a 5-mm-diameter spherical ROI was placed within normal-appearing white matter (NAWM) in T2 or FLAIR images, respectively, to acquire CBF data for normalization of DSC and ASL values in tumor regions.

Image Registration, Postprocessing, and Data Analysis

All images for each patient were registered to a high-resolution (1.0 mm isotropic), T1-weighted brain atlas (MNI152; Montreal Neurological Institute, Montreal, Canada) using a mutual information algorithm and a 12-degree of freedom transformation using FSL (FMRIB, Oxford, UK; http://www.fmrib.ox.ac.uk/fsl/). Fine registration (1-2 degrees and 1-2 voxels) was then performed using a Fourier transform-based, six degrees of freedom, rigid body registration algorithm followed by visual inspection to ensure adequate alignment. DSC and ASL estimates of CBF in tumor ROIs were normalized to that of normal appearing white matter (NAWM) by dividing mean values for tumor ROIs by mean values for the respective modalities in NAWM. Linear regression was performed for data extracted from tumor ROIs to determine if there was a significant linear relationship between DSC and ASL CBF measurements. The voxel-wise correlation between DSC and ASL measurements of CBF was assessed for all voxels, for all patients. A linear correlation with no intercept was used as a model for the voxel-wise correlation between DSC and ASL estimates of CBF, which was tested for statistical significance using chi-squared goodness of fit using a reduced chi-squared value, $\chi^2_{red,}$ as the test statistic (ie, variance of the residuals). Although relative CBV is the most common metric used to evaluate tumor vascularity, we chose to compare CBF estimates between DSC and ASL because ASL inherently provides quantification of absolute CBF.

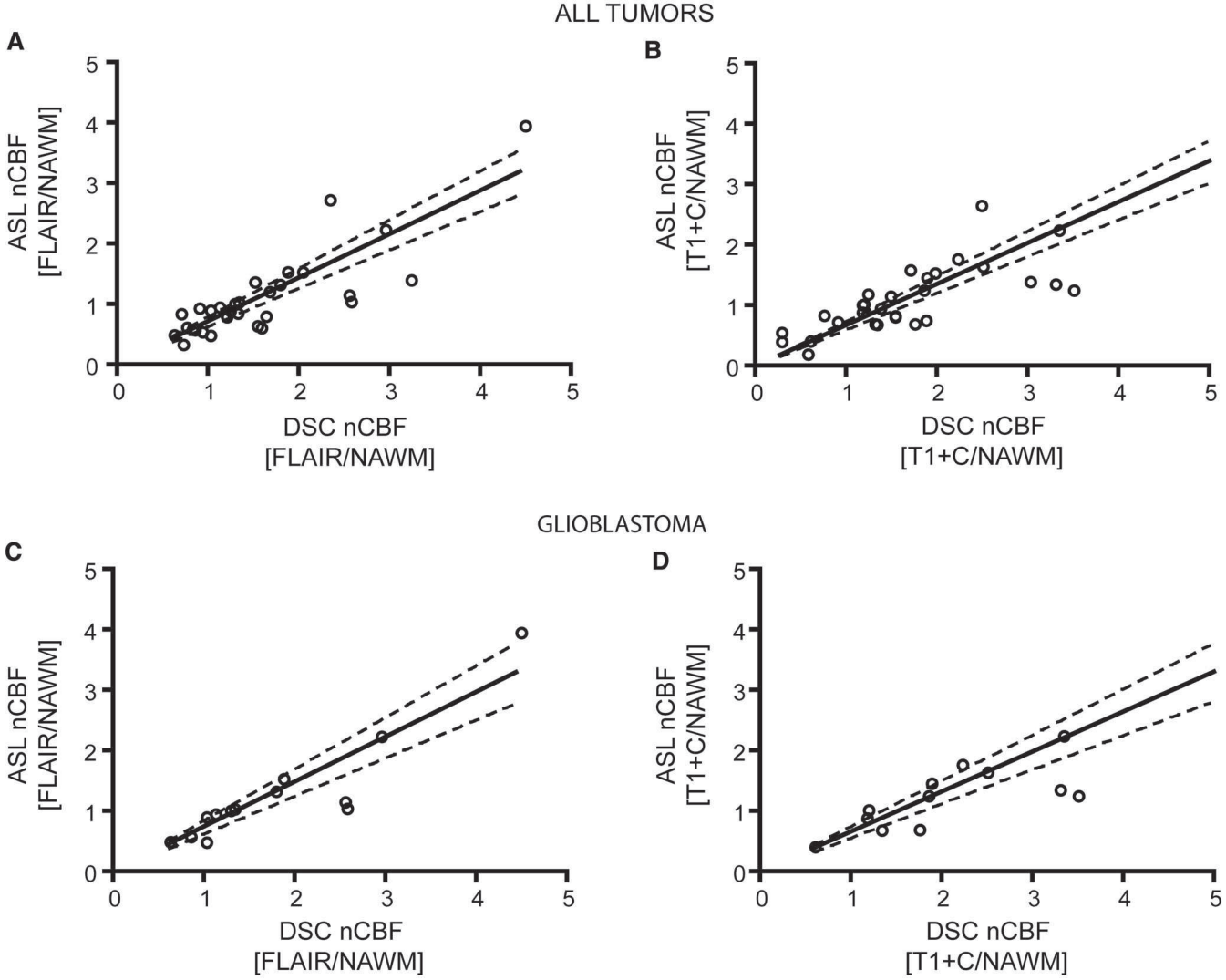

Fig 2. Patient-by-patient correlation between DSC and ASL measurement of mean white matter normalized cerebral blood flow (nCBF) measurements in regions of FLAIR and contrast-enhancement (T1+C). (A) ASL versus DSC measurements of nCBF within FLAIR hyperintense regions. (B) ASL versus DSC measurements of nCBF within contrast-enhancing regions (T1+C). (C) ASL versus DSC measurements of nCBF within FLAIR regions for glioblastoma patients. (D) ASL versus DSC measurements of nCBF within contrast-enhancing regions for glioblastoma patients.

Results

For most patients, DSC and ASL estimates of CBF were elevated within the areas of contrast-enhancement and the pattern of elevated CBF was similar between the two modalities. For example, Figure 1 illustrates a typical set perfusion images obtained in two different glioblastoma patients. In both these patients, the regions of contrast enhancement have the highest CBF; however, this elevated CBF is typically quite heterogeneous throughout the region of enhancement. As expected, both modalities show the lowest measured CBF within the central necrotic regions (hypointense on postcontrast T1-weighted images). ASL estimates of CBF, although quantitative and noninvasive in terms of exogenous contrast agent administration, were inherently of lower overall image quality compared to DSC estimates of CBF largely because of the low spatial resolution. Despite this disadvantage, ASL estimates of CBF appeared to be of sufficient quality to localize regions of highest vascularity when compared with DSC.

A statistically significant, positive linear correlation was observed between ASL and DSC estimates of mean normalized CBF within both FLAIR hyperintense (*Pearson's correlation coefficient,* $R^2 = .706$, $P < .0001$) and contrast-enhancing regions (*Pearson's correlation coefficient,* $R^2 = .809$, $P < .0001$) on a per patient basis (Figs 2A, B). The linear slope that best explained the correlation between normalized ASL and DSC estimates of CBF in all tumors was $.72 \pm .04$ standard error of the mean (SEM) for FLAIR hyperintense and $.68 \pm .03$ SEM for contrast-enhancing regions, suggesting DSC had about a 3:1 higher dynamic range of CBF measurements compared to ASL. Similarly for glioblastoma patients, a statistically significant linear was

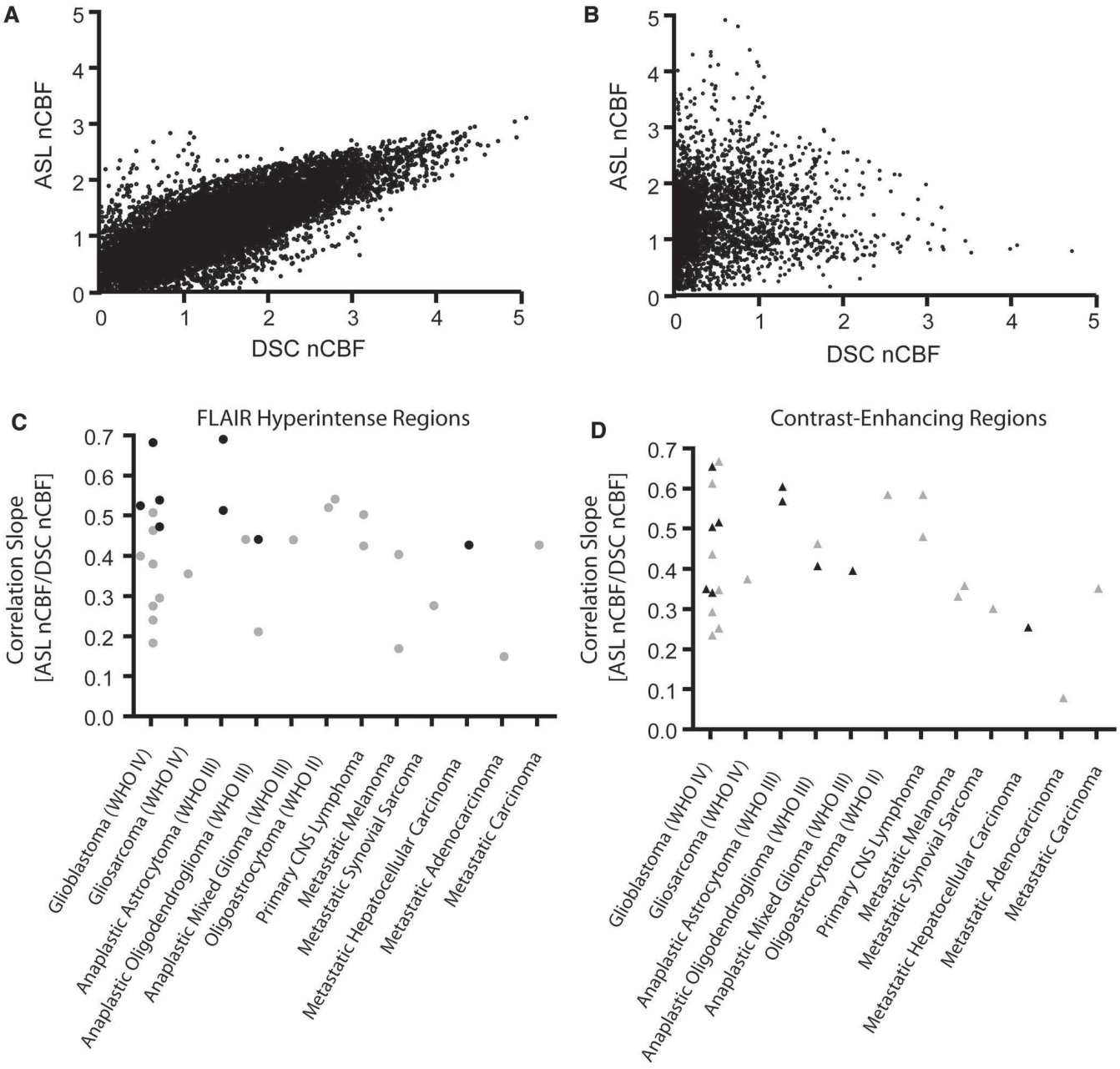

Fig 3. Voxel-wise correlation between white matter normalized cerebral blood flow (nCBF). (A) Voxel-wise correspondence between DSC and ASL measurements of nCBF within contrast-enhancing regions for a representative glioblastoma patient illustrating a strong linear correlation. (B) Voxel-wise correspondence between DSC and ASL measurements of nCBF within contrast-enhancing regions for a representative glioblastoma patient illustrating no linear correlation. (C) Slope of the best fit linear trend line between ASL and DSC measurements of nCBF within FLAIR hyperintense regions. (D) Slope of the best-fit linear trend line between ASL and DSC measurements of nCBF within contrast-enhancing hyperintense regions. Black marks represent statistically significant linear correlations according to Chi-squared goodness-of-fit tests. Gray marks represent other (nonsignificant) measurements.

observed in FLAIR (*Pearson's correlation coefficient,* $R^2 = .829$, $P < .0001$) and contrast-enhancing regions (*Pearson's correlation coefficient,* $R^2 = .872$, $P < .0001$). The linear relationship between ASL and DSC estimates of CBF in glioblastomas was similar to that of all tumors, measuring .74 ± .05 SEM for FLAIR and .66 ± .04 SEM for contrast-enhancing regions. These results suggest overall estimates of tumor blood flow may be similar between the two techniques, albeit to a different level of sensitivity and dynamic range.

Surprisingly, only a minority of patients examined in the current study demonstrated a statistically significant linear correlation between DSC and ASL measurements of relative CBF on a voxel-wise basis for areas of FLAIR and contrast-enhanced regions. As illustrated in Figure 3A, some patients did illustrate a strong voxel-wise association between the two measurements of CBF, specifically showing a 2:1 correspondence (slope ∼.5) between DSC and ASL DSC. The vast majority of patients, however, had voxel-wise relationships similar to those

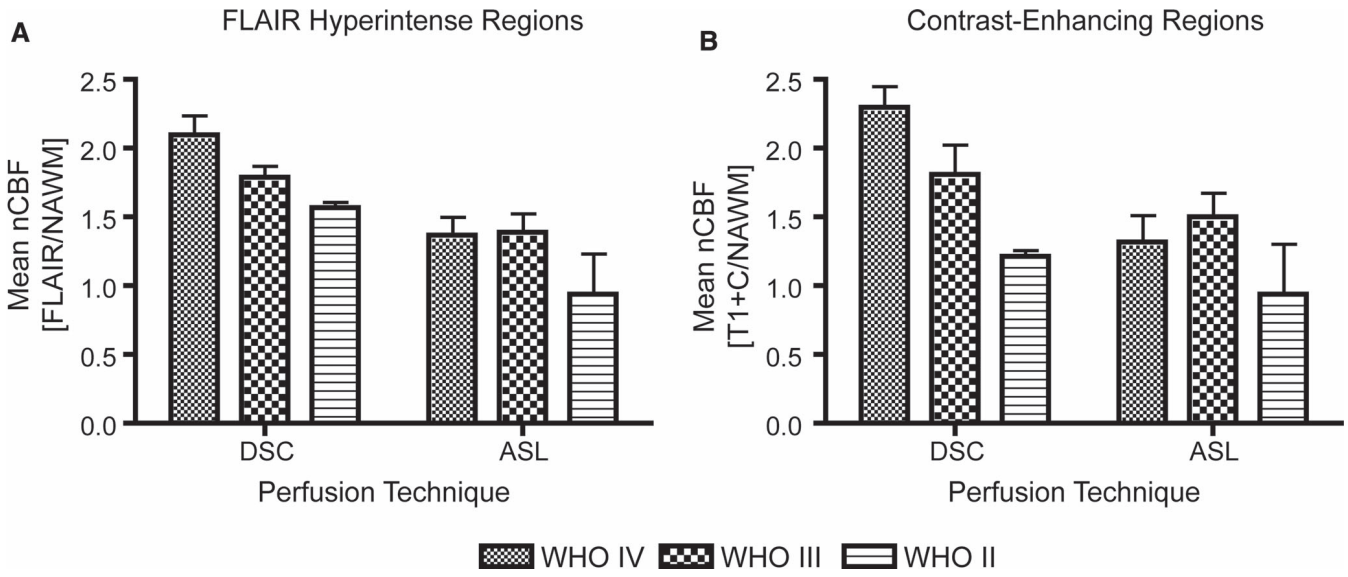

Fig 4. Mean white matter normalized cerebral blood flow (nCBF) for primary glioma patients stratified by WHO grade and evaluated between the two perfusion techniques. (A) nCBF measurements for DSC and ASL within FLAIR hyperintense regions. (B) nCBF measurements for DSC and ASL within contrast-enhancing (T1+C) regions.

illustrated in Figure 3B, where no apparent linear relationship was evident. Approximately 31% of glioblastoma patients (4 of 13) demonstrated a significant voxel-wise linear correlation between DSC and ASL measurements of CBF with FLAIR hyperintense regions and only 38% of glioblastoma patients (5 of 13) showed a significant correlation in contrast-enhancing regions (*Chi-Squared Goodness of Fit,* $\chi^2_{red} > 1.0$, $P < .05$). Interestingly, both patients with anaplastic astrocytoma (WHO III) had a significant voxel-wise correlation between DSC and ASL measurements of CBF in both FLAIR and postcontrast regions of interest (*Chi-Squared Goodness of Fit,* $\chi^2_{red} > 1.0$, $P < .05$). Also, metastatic hepatocellular carcinoma, a well-known highly vascular tumor, showed a statistically significant linear relationship between DSC and ASL measurements of CBF (*Chi-Squared Goodness of Fit,* $\chi^2_{red} > 1.5$, $P < .001$). Figures 3C and D illustrate the slope of the linear trend line for voxel-wise correspondence between DSC and ASL measurements within FLAIR and contrast-enhancing regions, respectively. Dark black symbols are those patients with statistically significant linear correlations between DSC and ASL measurements as measured using chi-squared goodness of fit analysis.

In general, patients with primary gliomas ($n = 22$) tended to have an increasing average normalized CBF for increasing WHO grade, suggesting higher cerebral blood flow in tumor regions with higher degree of malignancy (Fig 4). Surprisingly, there were clear differences in CBF measurements between WHO grades for DSC; however, ASL measurements were similar between WHO grades III and IV (malignant gliomas). In particular, results suggest a statistically significant difference between DSC and ASL estimates of normalized CBF for both FLAIR (*two-way ANOVA, DSC vs. ASL,* $P = .0027$) and contrast-enhancing regions (*two-way ANOVA, DSC vs. ASL,* $P = .035$). No statistically significant differences between WHO levels were found in FLAIR hyperintense regions (*two-way ANOVA, WHO grade,* $P = .10$), but significant differences were found between WHO levels inside contrast-enhancing regions (*two-way ANOVA, WHO grade,* $P = .040$); suggesting perfusion measurements within areas of contrast-enhancement may be the most useful for determining malignant potential.

Discussion

Our results demonstrate a positive linear correlation between DSC and ASL measurements of CBF from both FLAIR/T2 and postcontrast T1 weighted regions of interest on a patient-by-patient basis. This relationship is comparable to those reported in previous studies.[1,22,23] In addition, the correlation between DSC and ASL CBF values was higher in the subset of glioblastoma patients. This may be due to the fact that glioblastoma patients have an elevated CBF compared to other tumor types due to increased vascular proliferation and angiogensis.

In the current study we found no substantial voxel-wise correlation between DSC and ASL measurements in the majority of patients. There are several potential explanations for this observation. First, the use of gradient echo acquisition results in sensitivity to both small and large blood vessels,[24] which may be disproportionately represented in ASL estimates of CBF. In addition, previous investigations have shown that ASL underestimates CBF in brain regions with delayed arrival (eg, increased mean transit time), as would be the case with the tortuous vasculature from angiogenesis or regions of white matter where flow is low.[25,26] Alternatively, DSC remains relatively unaffected if postprocessing uses delay-invariant circular deconvolution methods are used,[24] as was the case in the current study. Another potential confound may be due to differences in the particular tracers employed in each modality. Because DSC uses a nondiffusible tracer, the tracer only accounts for a fraction of the volume of tissue of interest, in contrast to the diffusible tracer (ie, water) of ASL that distributes across capillary membranes throughout brain. CBF estimates are known to

differ between the two techniques simply due of the difference in diffusion behavior between the two tracers employed.[27] Additionally, calculations of DSC measurements assume that the tracer stays completely intravascular, which is not actually true in the case of high grade lesions and resultant blood brain barrier breakdown; however, in the current study we employed a preload along with posthoc leakage-correction algorithms.[2,8-10] Additionally, while great care was taken to properly align patient low resolution ASL data with high resolution anatomical and DSC data, misregistration between these data sets may have potentially confounded the voxel-wise coherence between the two modalities.

Implications on Clinical Care

Routine use of ASL for the assessment of brain tumor perfusion has not been established in the clinic, mostly due to relatively long acquisition times, lower image resolution, lower SNR, sensitivity to motion artifacts, and limited brain coverage. The advent of 3D PCASL with the use of background suppression at high field strengths has bridged this apparent gap, allowing higher resolution and higher SNR in shorter periods of time. Thus, the use of high resolution 3D PCASL with background suppression is a suitable option for evaluating brain tumor perfusion in patients with renal compromise; however, the administration of exogenous contrast agents remain the most advantageous image sequence for the clinical evaluation of brain tumors (eg, postcontrast T1-weighted images) and therefore the use of DSC-MRI during dynamic injection of contrast will remain an important sequence for evaluating tumor perfusion.

Grant Support:
UCLA Institute for Molecular Medicine Seed Grant (BME); UCLA Radiology Exploratory Research Grant (BME); Brain Tumor Funders Collaborative (WBP); Art of the Brain (TFC); Ziering Family Foundation in memory of Sigi Ziering (TFC); Singleton Family Foundation (TFC); Clarence Klein Fund for Neuro-Oncology (TFC).

References

1. Warmuth C, Gunther M, Zimmer C. Quantification of blood flow in brain tumors: comparison of arterial spin labeling and dynamic susceptibility-weighted contrast-enhanced MR imaging. *Radiology* 2003;228(2):523-532.
2. Boxerman JL, Schmainda KM, Weisskoff RM. Relative cerebral blood volume maps corrected for contrast agent extravasation significantly correlate with glioma tumor grade, whereas uncorrected maps do not. *AJNR Am J Neuroradiol* 2006;27(4):859-867.
3. Schramm P, Xyda A, Klotz E, et al. Dynamic CT perfusion imaging of intra-axial brain tumours: differentiation of high-grade gliomas from primary CNS lymphomas. *Eur Radiol* 2010;20(10):2482-2490.
4. Weber MA, Gunther M, Lichy MP, et al. Comparison of arterial spin-labeling techniques and dynamic susceptibility-weighted contrast-enhanced MRI in perfusion imaging of normal brain tissue. *Invest Radiol* 2003;38(11):712-718.
5. Kimura H, Takeuchi H, Koshimoto Y, et al. Perfusion imaging of meningioma by using continuous arterial spin-labeling: comparison with dynamic susceptibility-weighted contrast-enhanced MR images and histopathologic features. *AJNR Am J Neuroradiol* 2006;27(1):85-93.
6. Lu¨demann L, Warmuth C, Plotkin M, et al. Brain tumor perfusion: comparison of dynamic contrast enhanced magnetic resonance imaging using T1, T2, and T2$ contrast, pulsed arterial spin labeling, and H2(15)O positron emission tomography. *Eur J Radiol* 2009;70(3):465-474.
7. Lehmann P, Monet P, de Marco G, et al. A comparative study of perfusion measurement in brain tumours at 3 Tesla MR: arterial spin labeling versus dynamic susceptibility contrast-enhanced MRI. *Eur Neurol* 2010;64(1):21-26.
8. Schmainda KM, Rand SD, Joseph AM, et al. Characterization of a first-pass gradient-echo spin-echo method to predict brain tumor grade and angiogenesis. *AJNR Am J Neuroradiol* 2004;25(9):1524-1532.
9. Paulson ES, Schmainda KM. Comparison of dynamic susceptibility-weighted contrast-enhanced MR methods: recommendations for measuring relative cerebral blood volume in brain tumors. *Radiology* 2008;249(2):601-613.
10. Donahue KM, Krouwer HG, Rand SD, et al. Utility of simultaneously acquired gradient-echo and spin-echo cerebral blood volume and morphology maps in brain tumor patients. *Magn Reson Med* 2000;43:845-853.
11. Wu WC, M Fernandez-Seara, Detre JA, et al. A theoretical and experimental investigation of the tagging efficiency of pseudo-continuous arterial spin labeling. *Magn Reson Med* 2007;58(5):1020-1027.
12. Fernandez-Seara MA, Edlow BL, Hoang A, et al. Minimizing acquisition time of arterial spin labeling at 3T. *Magn Reson Med* 2008;59(6):1467-1471.
13. Wang J, Zhang Y, Wolf RL, et al. Amplitude-modulated continuous arterial spin-labeling 3.0-T perfusion MR imaging with a single coil: feasibility study. *Radiology* 2005;235(1): 218-228.
14. Herscovitch P, Raichle ME. What is the correct value for the brain–blood partition coefficient for water? *J Cereb Blood Flow Metab* 1985;5(1):65-69.
15. Kelly PJ, Daumas-Duport C, Scheithauer BW, et al. Imaging-based stereotaxic serial biopsies in untreated intracranial glial neoplasms. *J Neurosurg* 1987;66(6):865-874.
16. Kelly PJ, Daumas-Duport C, Kispert DB, et al. Stereotactic histologic correlations of computed tomography- and magnetic resonance imaging-defined abnormalities in patients with glial neoplasms. *Mayo Clin Proc* 1987;62(6):450-459.
17. Earnest FT., Kelly PJ, Scheithauer BW, et al. Cerebral astrocytomas: histopathologic correlation of MR and CT contrast enhancement with stereotactic biopsy. *Radiology* 1988;166(3):823-827.
18. Brant-Zawadzki M, Norman D, Newton TH, et al. Magnetic resonance of the brain: the optimal screening technique. *Radiology* 1984;152(1):71-77.
19. Tsuchiya K, Mizutani Y, Hachiya J. Preliminary evaluation of fluid-attenuated inversion-recovery MR in the diagnosis of intracranial tumors. *AJNR Am J Neuroradiol* 1996;17(6):1081-1086.
20. Essig M, Hawighorst H, Schoenberg SO, et al. Fast fluid-attenuated inversion-recovery (FLAIR) MRI in the assessment of intraaxial brain tumors. *J Magn Reson Imaging* 1998;8(4):789-798.
21. Ellingson BM, Cloughesy TF, Lai A, et al. Quantitative volumetric analysis of conventional MRI response in recurrent glioblastoma treated with bevacizumab. *Neuro Oncol* 2011;13(4):401-409.
22. Kimura T, Kusahara H. Reference-based maximum upslope: a CBF quantification method without using arterial input function in dynamic susceptibility contrast MRI. *Magn Reson Med Sci* 2009;8(3):107-120.
23. Jarnum H, Steffensen, EG, Knutsson L, et al. Perfusion MRI of brain tumours: a comparative study of pseudo-continuous arterial spin labelling and dynamic susceptibility contrast imaging. *Neuroradiology* 2010;52(4):307-317.

24. Boxerman J. L., Hamberg, LM, Weisskoff RM, et al. MR contrast due to intravascular magnetic susceptibility perturbations. *Magn Reson Med* 1995;34(4):555-566.
25. Petersen ET, Zimine I, Ho YC, Golay X. Non-invasive measurement of perfusion: a critical review of arterial spin labelling techniques. *Br J Radiol* 2006;79:688-701.
26. van Gelderen P, de Zward JA, Duyn JH. Pitfalls of MRI measurement of white matter perfusion based on arterial spin labeling. *Magn Reson Med* 2008;59:788-795.
27. Ye FQ, KF Berman, Ellmore T, et al. H(2)(15)O PET validation of steady-state arterial spin tagging cerebral blood flow measurements in humans. *Magn Reson Med* 2000;44(3):450-456.